IL-17A both initiates (via IFNγ suppression) and limits the pulmonary type 2 immune response to nematode infection

Short title: IL-17A regulates pulmonary type 2 immunity

Jesuthas Ajendra[1], Alistair L. Chenery[1], James E. Parkinson[1], Brian H. K. Chan[1], Stella Pearson[1], Stefano A. P. Colombo[1], Louis Boon[2], Richard K. Grencis[1], Tara E. Sutherland[1]*, Judith E. Allen[1]*

* Joint corresponding

Correspondence:

Tara E. Sutherland

tara.sutherland@manchester.ac.uk

The University of Manchester, Core Technology Facility, Grafton St, Manchester, M13 9NT United Kingdom

Tel: +44 161 306 6052

Judith E. Allen

judi.allen@manchester.ac.uk

The University of Manchester, AV Hill Building, Oxford Road, Manchester, M13 9PT, United Kingdom.

Tel: +44 161 306 1347

[1] Lydia Becker Institute for Immunology & Infection, Wellcome Centre for Cell-Matrix Research, Faculty of Biology, Medicine & Health, Manchester Academic Health Science Centre, University of Manchester, Manchester, United Kingdom

[2] Bioceros, Member of Polpharma Biologics, Yalelaan 46, 3584 CM Utrecht, The Netherlands

The authors declare no conflicts of interest.

Abstract

Nippostrongylus brasiliensis is a well-defined model of type 2 immunity but the early lung-migrating phase is dominated by innate IL-17A production and neutrophilia. While the importance of IL-17A is well established during microbial infections, its contribution to type 2 immunity is poorly understood. Using *N. brasiliensis* infection we show that *Il17a*-KO mice exhibited an impaired type 2 immune response correlating with increased worm burden. Neutrophil depletion and reconstitution studies demonstrated that neutrophils contributed to the subsequent eosinophilia but were not responsible for the ability of IL-17A to promote type 2 cytokine responses. Transcriptional profiling of the lung on day 2 of *N. brasiliensis* infection revealed an increased IFNγ signature in the *Il17a*-KO mice confirmed by enhanced IFNγ protein production. Depletion of early IFNγ restored type 2 immune responses in the *Il17a*-KO mice supporting the hypothesis that the suppression of IFNγ by innate IL-17A sources promotes the protective type 2 immune response. Notably, when IL-17A was blocked later in infection, there was an increased type 2 response. Combined data from both *N. brasiliensis* and *Trichuris muris*, a gut-specific pathogen, demonstrated that IL-17A regulation of type 2 immunity was lung-specific. Together our data suggest that IL-17A is a major regulator of type 2 immunity in the lung which supports the development of a protective type 2 immune response but subsequently limits the magnitude of that response.

Introduction

Innate and adaptive sources of interleukin-17A (IL-17A) are responsible for a range of neutrophil-associated inflammatory conditions as well as protection from many bacterial and fungal pathogens [1] [2]. In contrast, type 2 immunity is required for effective control of most helminth infections [3] and is characterized by eosinophilic inflammation and the cytokines IL-4, IL-5 and IL-13. When both type 2 and IL-17 responses are present during helminth infection enhanced pathology is observed, as shown for human schistosomiasis [4], [5] and onchocerciasis [6]. The detrimental relationship between IL-17A and type 2 associated diseases has also been extensively documented in allergic asthma in which the most severe symptoms occur in patients with both high Th2 and Th17 cell responses [7]. Critically, type 2 cytokines can actively suppress IL-17A production which may be an important feedback mechanism to avoid extreme IL-17A-driven pathology [8]–[10]. Despite the evidence for an important

relationship between IL-17A and type 2 immune responses during chronic disease, how these responses are connected remains poorly understood.

We and others have demonstrated a prominent role for IL-17A during infection with the lung-migrating nematode *Nippostronglyus brasiliensis* [8][11], a well-defined pulmonary model of type 2 immunity. After entering the host via the skin, *N. brasiliensis* larvae migrate through the blood vessels into the lung, causing tissue damage and haemorrhage. IL-17RA-dependent neutrophil recruitment is largely responsible for the lung damage in this model [12]. We previously found that the chitinase-like protein Ym1 induces expansion of IL-17A-producing γδ T cells and Ym1 blockade or IL-17A-deficiency protects mice from peak lung damage [8]. More surprising was our finding that Ym1 neutralisation or IL-17A-deficiency prevents the development of a full type 2 response during *N. brasiliensis* infection [8], [13].

The notion that IL-17A is required for development of a type 2 response appears counter to the evidence that type 2 cytokines suppress IL-17A production[9], [10]. However, previous studies using murine models of allergic inflammation also show impaired type 2 immunity in the face of IL-17A deficiency [14], [15] or blockade [16]. In an infection or injury context, the specific tissue as well as timing might all play decisive roles in whether IL-17A augments or suppresses type 2 responses. We therefore used *N. brasiliensis* infection to address the contribution of γδ T cell-derived IL-17A and neutrophils to the development of a subsequent type 2 immune response in the lung. We found that IL-17A suppressed early IFNγ production and that this suppression was essential for the optimal development of a type 2 response. Although neutrophils acted as a major driver of subsequent lung eosinophilia, neutrophils were not responsible for IL-17A-mediated enhancement of type 2 immunity. Once the type 2 response was established, IL-17A acted as a negative regulator, revealing distinct roles during innate and adaptive stages of the response. Notably, *Trichuris muris,* a nematode restricted to the gastro-intestinal tract also induced a lung type 2 response that was IL-17A-dependent. However, we found no evidence that IL-17A regulated the intestinal type 2 response. Thus, IL-17A serves as a lung-specific regulator of the type 2 immune response.

Materials & Methods

Mice and ethics statement

For experiments using only WT mice, C57BL/6 J mice were obtained from Charles River. C57BL/6 *Il17a*^{Cre}*Rosa26*^{eYFP} mice were originally provided by Dr Brigitta Stockinger[17], [18]. For *Il17a*-KO experiments C57BL/6 WT mice and C57BL/6 *Il17a*^{Cre}*Rosa26*^{eYFP} homozygote mice were bred at the University of Manchester. Mice were age- and sex-matched and all mice were housed in individually ventilated cages. Both males and females were used. Mice were not randomized in cages, but each cage was randomly assigned to a treatment group. Mice were culled by asphyxiation in a rising concentration of CO_2. Experiments were performed in accordance with the United Kingdom Animals (Scientific Procedures) Act of 1986.

N. brasiliensis infection.

N. brasiliensis was maintained by serial passage through Sprague-Dawley rats, as described [19]. Third-stage larvae (L3) were washed ten times with PBS (Dulbecco's PBS, Sigma) before infection. On day 0, mice were infected subcutaneously with 250 or 500 larvae (L3). At various time points mice were euthanised, bronchoalveolar lavage (BAL) was performed with PBS containing 1% BSA and lungs were taken for further analysis. For worm counts, the small intestines of infected mice were collected in PBS. Small intestines were then cut longitudinally along the entire length, placed in a 50 ml Falcon and incubated at 37°C for 4h. Settled worms were then counted with the aid of a dissecting microscope.

Flow cytometry.

Single-cell suspensions of the lung were prepared by digesting minced lung lobes for 30 min at 37 °C with 0.2 U/ml Liberase TL (Roche) and 80 U/ml DNase (Life Tech) in Hank's balanced-salt solution before forcing tissue suspensions through a cell strainer (70 µm, Greiner). Red blood cells were lysed using Red Blood Cell Lysing Buffer Hybri Max (Sigma) for 3 min at RT and reaction was stopped by diluting samples in PBS. Total live cells were counted with AO/PI dye on an automated cell counter (Auto2000, Nexcelom). Cells were stained for live/dead (Life Technologies) and then incubated with Fc block (1:500 CD16/CD32 and 1:50 mouse serum) and were then stained with fluorescence-conjugated antibodies. Cells were identified by expression of surface markers as follows:

neutrophils Ly6G$^+$CD11b$^+$, eosinophils CD11b$^+$ CD11c$^-$ SigF$^+$, CD4 T cells CD4$^+$, TCRβ$^+$CD11b$^-$, γδ Tcells TCRβ$^-$, TCRγδ$^+$, CD11b$^-$ and ILC2s Lineage$^-$ (CD11b, TCRβ, TCRγδ, Ly6G, F4/80, CD11c, SigF, CD19) CD90.2$^+$KLRG$^+$CD127$^+$. Antibody clones used are listed in **Table 1**. For staining of intracellular cytokines, cells were stimulated for 4 h at 37 °C with cell stimulation cocktail containing protein transport inhibitor (eBioscience), then stained with live/dead. After surface antibody staining, cells were fixed for 10 min at 4 °C using IC fix (Biolegend) and cells were then incubated in for 20min at RT in Permeabilization buffer (biolegend). Intracellular staining was performed for cytokines using antibodies for IL-5, IL-13, IL-17A and IFNγ as well as for YM1 and Relm-α. Samples were analysed by flow cytometry with LSR Fortessa or LSR II (Becton-Dickinson) and data analysed using FlowJo v10 software.

Table 1 List of flow cytometry antibodies used.

Antigen	Clone	Manufacturer
CD11b	M1/70	BioLegend
CD11c	N418	BioLegend
Ly6C	HK1.4	BioLegend
CD4	GK1.5	BioLegend
F4/80	BM8	eBioscience
CD90.2	30-H12	Biolegend
CD127	A7R34	Invitrogen
KLRG1	2F1	Biolegend
TCRβ	H57-597	BioLegend
TCRγδ	GL3	BioLegend
ST2	DIH9	BioLegend
IL-5	TRFK5	BioLegend
IL-17A	TC11-18H10.1	BioLegend
Ly6G	1A8	BD Biosciences
Siglec-F	E50-2440	BD Biosciences
F4/80	BM8	ThermoFisher
IL-13	eBio13A	ThermoFisher
Ym1	Polyclonal	R&D Systems
RELM-α	Polyclonal	Peprotech
IFNγ	XMG1.2	Biolegend
CD69	H1.2F3	Biolegend
EGFR	EGFR1	Abcam

Quantification of cytokines.

Single-cell suspensions of splenocytes, lung-draining lymph nodes or whole lung were stimulated *ex vivo* with *N. brasiliensis* excretory secretory product (E/S) antigen [20] (1 µg/ml) or anti-CD3 (1 µg/ml). Cell supernatants were harvested 72 h later and were stored at −20 °C until further analysis. Mouse IL-13 DuoSet ELISA kit (R&D Systems) was used for measurement of IL-13 levels. Mesenteric lymph node (MLN) cells from *T. muris* infected or uninfected mice were collected, cultured and restimulated *ex vivo* for 36 h with E/S as previously described [21]. The concentrations of IL-5, IL-6, IL-9, IL-10, IL-13, IL-17A, TNFα and IFNγ in the MLN culture supernatant were measured by cytokine bead array (CBA, BD Biosciences, UK) as per the manufacturer's protocol.

Antibody depletion and cell transfer experiments

Neutrophils were depleted via intraperitoneal injection of anti-Ly6G antibody (clone 1A8, BioXcell, West Lebanon, NH, USA) (500 µg/mouse/day) on days -1 and 1 of infection with *N. brasiliensis*. Control mice were injected with an equal volume of IgG2a isotype control (BioXcell). Neutrophil depletion was confirmed by anti-Gr1 (RB6-8C5) staining for flow cytometry. For neutrophil transfer, neutrophils were purified from bone marrow using Histopaque-based density gradient centrifugation as described before [22]. Collected neutrophils were washed twice with RPMI 1640 and counts and viability was determined (average purity 85% ± 4.42% and 90% ± 1.5% viability). Neutrophils were resuspended in PBS and 0.5 x 10^6 cells (40µl) transferred intranasally into mice on day 1 post infection with *N. brasiliensis*. IFNγ was depleted using an anti-IFNγ monoclonal antibody (clone XMG1.2) and injected intraperitoneally (500 µg/mouse/day) on days -1 and 1 of infection with *N. brasiliensis*. Control mice were injected with an equal amount of corresponding isotype control (GL113). IL-17A was depleted using an anti-IL-17A (17F3) or IgG1 isotype (both Invivo mAB) injected intraperitoneally (100 µg/mouse/day) on days 4, 5 and 6 post-infection with *N. brasiliensis*.

Histology

For histology, the left lobe of the lung was isolated at different time points following *N. brasiliensis* infection, inflated and fixed in 10% neutral-buffered formalin (Sigma). Whole left lung lobes were processed using a tissue processor (Leica ASP300S) and were then embedded in paraffin. Paraffin blocks were then sectioned to 5 µm using a microtome (Leica

RM2235) and routinely stained with Mayer's haematoxylin (Merck Millipore HX86014349) and eosin (Sigma) for histological analysis. Slides were imaged using an Olympus slide scanner and high-resolution image files were exported using Pannoramic Viewer software (3DHISTECH). The images were then processed in a KNIME software workflow to obtain 50 random regions of interests (ROIs) across the whole lung section. ROIs that contained lobe boundaries or extensive artefacts were excluded from the analysis. The ROIs were then converted to binary images and lacunarity (Λ) was quantified using the FracLac plugin for ImageJ. The Λ values of all the ROIs were averaged to obtain estimates for the entire lobe.

Extraction of RNA and quantitative real-time PCR

A fragment of the right lung lobe was stored in RNAlater (Ambion) before homogenization of tissue in Qiazol reagent with a TissueLyser (Qiagen). RNA was prepared according to manufacturer's instructions. RNA was quantified using a ND-1000 Spectrophotometer (NanoDrop Technologies). Reverse transcription of 1 µg of total RNA was performed using Tetro reverse transcriptase (Bioline). For reverse transcription, total RNA was treated with 50 U Tetro reverse transcriptase (Bioline), 40 mM dNTPs (Promega), 0.5 µg PolyT primer for cDNA synthesis (Roche) and RNasin inhibitor (Promega). The abundance of transcripts from the genes of interest was measured by quantitative real-time PCR with the Light Cycler 480 II system (Roche) with a Brilliant III SYBR master mix (Agilent) and specific primer pairs. PCR amplification was analysed by the second-derivative maximum algorithm (Light Cycler 480 Sw 1.5; Roche), and expression of the gene of interest was normalized to that of the housekeeping gene *Actb* (beta-actin). A list of primer sequences used are shown in **Table 2**.

Table 2 List of primer sequences used.

Primer	**Sequence (5'-3')**
Ccl8 forward	TTCTTTGCCTGCTGCTCATA
Ccl8 reverse	AGCAGGTGACTGGAGCCTTA
Il5 forward	ACATTGACCGCCAAAAAGAG
Il5 reverse	CACCATGGAGCAGCTCAG
Chil3 forward	ACCTGCCCCGTTCAGTGCCAT
Chil3 reverse	CCTTGGAATGTCTTTCTCCACAG
Il4 forward	CCTGCTCTTCTTTCTCGAATGT
Il4 reverse	CACATCCATCTCCGTGCAT

Retnla forward	TATGAACAGATGGGCCTCCT
Retnla reverse	GGCAGTTGCAAGTATCTCCAC
Il13 forward	CGTTGCACAGGGGAGTCT
Il13 reverse	CCTCTGACCCTTAAGGAGCTTAT
Ifng forward	GGAGGAACTGGCAAAAGGAT
Ifng reverse	TTCAAGACTTCAAAGAGTCTGAGG
Actb forward	GCCGGACTCATCGTACTCC
Actb reverse	GTGACGTTGACATCCGTAAAG
Muc5ac forward	GCATCAATCAACAGCGAAACTT
Muc5ac reverse	CGAGTCACCCCCTGAGTC
Muc5b forward	GAGGTCAACATCACCTTCTGC
Muc5b reverse	TCTCATGGTCAGTTGTGCAGG

Trichuris muris infection and E/S products

T. muris eggs were prepared from chronically infected stock mice as described previously [23]. Mice were infected by oral gavage with 200 embryonated *T. muris* eggs suspended in ddH2O. At day 20 and 35 post infection, *T. muris* burden was assessed by removing the caecum and proximal colon, opening them longitudinally and scraping the contents out with fine forceps. Individual worms were then counted by eye under a binocular dissecting microscope. *T. muris* adult excretory secretory product antigen (E/S) was prepared as described by [23]. In brief, adult *T. muris* were cultured *ex vivo* at 37^{o}C, the culture supernatant was collected and centrifuged to remove eggs and worms. The resultant supernatant was then filter sterilised and stored at -20^{o}C until use for *in vitro* re-stimulation of MLN cells.

Nanostring RNA Profiling

Samples were run on an Agilent 2200 Tape Station system to ensure high quality lung RNA; samples with a RIN value of < 6.5 were excluded. RNA was diluted to 20ng/µL in RNase free H_2O, measured using Qubit™ RNA HS Assay Kit (Thermofisher) and run on a Nanostring nCounter® FLEX system using the Myeloid Innate Immunity v2 panel (XT-CSO-MMII2-12) as per manufacturer's instructions. Raw data was loaded into nSolver version 4.0 using default settings. non-normalised counts were then exported and subsequent analyses were performed in R (version 3.6) [24] using RStudio Version 1.2.1335 Build 1379 – © 2009-2019 RStudio, Inc. Positive controls were analysed to ensure there was clear resolution at variable expression

levels and negative controls were used to set a minimum detection threshold which was applied to all samples. Data were then normalised with EdgeR [25] using the TMM method and differential expression between *N. brasiliensis*-infected WT and IL-17A-deficient mice was calculated via linear modelling with Empirical Bayes smoothing using the limma R package 2. Heatmaps were then generated from normalized counts of differentially expressed genes using the ComplexHeatmaps R package [26]. The networks and functional analyses of differentially expressed genes were generated with Ingenuity pathway analyser (QIAGEN Inc., https://www.qiagenbio-informatics.com/products/ingenuity-pathway-analysis). Data were then imported into R for visualisation [27].

Statistical analysis.

Prism 7.0 (version 7.0c, GraphPad Software) was used for statistical analysis. Differences between experimental groups were assessed by ANOVA (for normally distributed data, tested using Shapiro-Wilk normality test) followed by Sidak's multiple comparisons test. For gene expression data, values were $\log_2$ transformed to achieve normal distribution. Comparisons with a *P* value of less than 0.05 were considered to be statistically significant.

Results

IL-17A-deficient mice mount a diminished type 2 response

In keeping with the known ability of *N. brasiliensis* to induce a strong pulmonary type 2 immune response on day 6 post infection (d6pi), we found the BAL and lungs of C57Bl/6 mice to be dominated by eosinophils (Suppl. Fig. 1A, B). This response was accompanied by elevated numbers of $CD4^+$ T cells as well as induction of Group 2 Innate lymphoid cells (ILC2, Suppl. Fig. 1C, D). The establishment of a type 2 response was further confirmed by increased type 2 cytokine expression by $CD4^+$ T cells and gene expression in whole lung (Suppl. Fig. 1E, F). As we and others previously reported [8], [11] infected mice exhibited increased IL-17A production in the first 48 h post infection (Fig. 1A) and consistent with previous reports the main source of IL-17A was γδ T cells [8]. On d2pi the BAL consisted mainly of neutrophils (Suppl. Fig.1A), which, together with *N. brasiliensis* larvae migration, is known to cause acute lung injury responses [11].

To investigate the role of IL-17A during the development of type 2 immune responses, we infected *Il17a*-KO mice and corresponding WT C57BL/6J controls with *N. brasiliensis* L3's.

Larvae leave the lung within 48 h and are expelled from the gut within 6-8 days. Consistent with our previous findings [8] *Il17a*-KO mice were significantly more susceptible to infection exhibiting an intestinal worm burden almost twice as high as in the WT controls on d4pi and d6pi Fig. 1B). As expected, the early d2 neutrophilia in response to *N. brasiliensis* infection was muted in the *Il17a*-KO mice relative to the WT controls (Fig. 1C). Between day 2 and 6 post infection, there was a switch from neutrophilic to eosinophilic responses in the lungs (Suppl. Fig 1A). Whilst increased eosinophil numbers were observed in all infected d6pi mice relative to naïve animals, this increase was less evident for *Il17a*-KO mice (Fig. 1D). ILC2 displayed a similar pattern, as cell numbers significantly increased with infection in WT but not in *Il17a-KO* mice (Fig. 1E). Additionally, WT mice exhibited an increased type 2 cytokine expression signature at d6pi, whilst *Il17a*-KO mice had reduced *Il4* expression and a significantly delayed increase in *Il5* expression (Fig. 1F). IL-13 protein levels in whole lung samples restimulated with α-CD3 on d6pi were significantly higher in WT mice compared to naïve controls whilst *Il17a*-KO mice completely failed to upregulate IL-13 levels (Fig. 1G), further demonstrating an impairment of protective type 2 responses. We also measured expression levels of the major mucins in the lung because host mucin production is another feature of anti-helminth protective type 2 responses [28]. *N. brasiliensis* infection drove an early increase in mucins *Muc5ac* and *Muc5b* expression in the lungs of WT mice at day 2 post-infection corresponding to a time when the larvae are transitioning from the lungs. Expression of the mucin *Muc5ac* was significantly increased in WT mice compared to naïve controls, but reduced in *Il17a*-KO mice, although not significant (Fig. 1H). A similar pattern was observed for *Muc5b* expression, which was upregulated in infected WT mice by day 2, but failed to increase in *Il17a*-KO infected mice (Fig. 1H). By d6pi, when the worms had already migrated to the small intestines, increased mucin expression was no longer observed in infected animals (Fig. 1H). Together these data demonstrate an impairment of type 2 immune responses during helminth infection in the absence of IL-17A.

IL-17A regulates T cell activation and polarization during *N. brasiliensis* infection

Next we aimed to determine whether the impact of IL-17A-deficiency on type 2 immunity was due to changes in T cell activation or polarisation during *N. brasiliensis* infection. Using flow cytometry, we observed a reduction in total numbers of $CD4^+$ T cells on d7pi in the lungs of *Il17a*-KO mice compared to WT controls (Fig. 2A). In contrast, there were no significant differences in $CD4^+$ T cell numbers in the lung-draining lymph nodes (Fig. 2A).

Not only were there fewer $CD4^+$ T cells in the lungs of *Il17a*-KO mice, the $CD4^+$ T cells of *Il17a*-KO mice were producing significantly less IL-13 and IL-5 (Fig. 2B). We also found significantly fewer $IL\text{-}5^+$ and $IL\text{-}13^+$ $CD4^+$ T cells in the *Il17a*-KO mice compared to WT controls (Fig. 2C). At the same time point post-infection, we found that expression of the activation marker CD69 was upregulated in the lungs of WT but not *Il17a*-KO mice (Fig. 2D). However, CD69 did not differ between all tested groups in the lung-draining lymph nodes (Fig. 2E). Recently, Minutti et al. described a role for epidermal growth factor receptor (EGFR) on T cells in protection against *N. brasiliensis*. EGFR forms a complex with ST2 to allow for IL-33-induced IL-13 expression at the site of infection [29]. We therefore analysed surface expression of EGFR and ST2 on lung and lung-draining lymph node T cells. *N. brasiliensis* infection increased the number of $CD4^+$ T cells expressing these markers in the lung, but this increase was significantly reduced in *Il17a*-KO mice. (Fig. 2D). Changes to ST2 and EGFR expression between WT and KO mice were not observed in the lung-draining-lymph nodes (Fig. 2E). We also measured PD-1 expression, an important regulator of T cell function during helminth infection [30], [31]. *N. brasiliensis* infection in WT mice led to increased numbers of $CD4^+$ T cells expressing PD-1 in the lung (Fig. 2D) with significantly fewer of these cells in *Il17a*-KO mice (Fig. 2D). Whilst there were also increased numbers of $PD\text{-}1^+CD4^+$ T cells in the lymph node following infection of WT mice, these were not altered by the absence of IL-17A (Fig. 2D). Overall, these data demonstrate the lung-specific impact of IL-17A-deficiency on $CD4^+$ T cell numbers, type 2 cytokine production and activation status.

Neutrophils regulate eosinophil recruitment but not type 2 responses

IL-17A is a major driver for neutrophil recruitment and activation [32], raising the possibility that impaired neutrophilia in *Il17a*-KO mice is responsible for diminished type 2 immune responses. This hypothesis was supported by data indicating that neutrophils from *N. brasiliensis* infected mice can express type 2 cytokines [11]. Therefore, we assessed whether neutrophils contributed to the type 2 immune response by depleting neutrophils during *N. brasiliensis* infection (Fig. 3A). Injection of anti-Ly6G effectively prevented neutrophil accumulation in the BAL at d2pi compared to isotype control and depletion was still evident in the blood at d6pi (Fig. 3B, Suppl. Fig. 2A). Neutrophilia at day 2 post *N. brasiliensis* infection is a major driver of the lung injury [11] and here we confirmed these findings (Fig. 3C). Histological sections demonstrated infection-induced injury at d2pi in isotype-treated WT mice, an effect that is almost absent in infected mice depleted of neutrophils. Using lacunarity

[33] as an indicator of acute lung injury [34], we show that neutrophil depleted mice show no significant signs of damage (Fig. 3C). Whilst intestinal worm burdens at d2pi and d4pi were not affected by neutrophil depletion, a small but significant increase in parasite numbers at d6pi was observed in mice treated with neutrophil-depleting antibody (Fig. 3D). As expected, eosinophils were prominent in the lung and BAL of isotype-treated mice at d6pi (Fig. 3E). However, depletion of neutrophils in infected mice significantly reduced eosinophils in the lung and BAL compared to the isotype-treated animals. Notably, blood and bone marrow eosinophils were not affected, suggesting a defect in eosinophil recruitment (Supplement Fig. 2B). We therefore assessed chemokines with known eosinophil chemotactic effects (*Ccl5, Ccl11*, *Ccl22*), but neutrophil-depletion did not alter mRNA expression of these chemokines in the lung. In addition, we measured *Ccl8* as Chen et al. demonstrated that *N. brasiliensis*-primed neutrophils from d2pi exhibit a notable upregulation of *Ccl8* [11]. Expression of *Ccl8* was increased in infection, but significantly lower in neutrophil-depleted mice (Suppl. Fig. 2C). As expected, *N. brasiliensis* infection significantly increased $CD4^+$ T cells in the lung, but the number of $CD4^+$ T cells were significantly reduced following neutrophil depletion (Fig. 3F). Despite effects on both $CD4^+$ T cells and eosinophilia, there were limited changes in type 2 cytokine expression following neutrophil depletion (Fig, 3G, H). Whilst IL-4 levels significantly increased in infected isotype treated mice, there was no significant upregulation of IL-4 expression in whole lung or by $CD4^+$ T cells in neutrophil-depleted mice (Fig. 3G-H). IL-13 and IL-5 were not also altered (Fig. 3G, H, Suppl. Fig. 2D). Thus, neutrophil depletion prevented eosinophil recruitment to the lungs of infected mice, but had a limited effect on type 2 cytokine expression.

To further address the role of neutrophils, we tested whether transfer of WT neutrophils into *Il17a*-KO mice could rescue the defect in the development of type 2 immunity. Neutrophils were isolated from the bone marrow of $CD45.1^+$ mice using the histopaque-gradient method [22] and intranasally transferred into *Il17a*-KO mice (Fig. 3I). Neutrophil transfer restored airway neutrophil frequency in *Il17a*-KO mice (Fig. 3J). Interestingly, this neutrophilic response was due to increased recipient-derived cells and not the transferred $CD45.1^+$ neutrophils (Suppl. Fig. 2E). One day post-neutrophil transfer (on d2pi), eosinophil numbers were increased in *Il17a*-KO mice, reaching similar numbers to those observed in infected WT mice (Fig. 3K). *Ccl8* levels were also increased following neutrophil transfer (Suppl. Fig. 2F), consistent with the possibility that this chemokine plays a role during eosinophil recruitment to site of infection. At a later timepoint, when eosinophilia was much more dominant and pronounced, the *Il17a*-KO mice that received neutrophils also displayed an increased lung

eosinophilia (Fig. 3L). Despite changes to eosinophil numbers, transfer of neutrophils did not rescue the deficit in type 2 cytokines in *Il17a*-KO mice (Fig. 3M). Together, this data provides evidence that neutrophils support eosinophil recruitment at the site of infection, but suggests they do not directly contribute to type 2 cytokine responses.

IL-17A leads to a downregulation of early IFNγ during *Nippostronglyus* infection

Rapid early IL-17A production is known to be critical for protective immune responses in different settings of lung immunity [1], [35]. To better understand the early events unfolding in the lung during *N. brasiliensis* infection, we performed a Nanostring gene expression array using a myeloid immunity panel (700 genes). Differentially expressed (DE) genes in whole lung between naïve WT mice and infected WT and *Il17a*-KO mice at d2pi were assessed in total unamplified RNA (Fig 4A). IL-17A deficiency led to a distinct gene expression profile compared to WT mice in response to *N. brasiliensis* infection. Notably, when analysing all DE genes (Fig. 4A) using the Ingenuity pathway analyser (Qiagen), IFNγ was predicted as the most significantly increased upstream regulator in *N. brasiliensis* infected *Il17a*-KO compared to WT mice (Fig. 4B). This led us to hypothesize that IL-17A may suppress IFNγ, which would facilitate Th2 cell development and explain why mice deficient in IL-17A cannot induce a full type 2 immune response. This hypothesis was also consistent with our unpublished and published [36] finding that Ym1, which induces IL-17A, strongly suppresses IFNγ. To test this possibility, we assessed IFNγ responses in *Il17a*-KO mice after *N. brasiliensis* infection. While WT mice exhibited significant suppression of *Ifng* in whole lung at 2dpi compared to uninfected controls, mice deficient in IL-17A did not show this phenotype (Fig. 4C). By intracellularly staining for IFNγ, we observed that *Il17a*-KO mice infected with *N. brasiliensis* failed to exhibit the early downregulation of IFNγ expression seen in infected WT mice (Fig. 4D). Importantly, this failure of suppression was observed across different types of IFNγ-producing cells. Lung $CD4^+$ T cells, $CD8^+$ T cells as well γδ T cells from *Il17a*-KO mice produced IFNγ at the same proportion as the naïve controls, while WT mice exhibited a downregulation in IFNγ production (Fig. 4D). We further assessed whether early IFNγ was produced by γδ T cell subsets that differ in their expression of CD27 and CD44 [37]. At 16 h post *N. brasiliensis* infection, IFNγ frequencies were also significantly increased in γδ T cells of *Il17a*-KO mice compared to WT controls (Fig. 4E). Consistent with expectations [37], the $CD27^+$ γδ T cells were the main producers of IFNγ after infection (Fig. 4F). Overall, our data demonstrated that IL-17A-deficiency enhanced IFNγ production during infection, supporting

the hypothesis that IL-17A plays an important role in downregulating IFNγ at the site of infection during the lung migratory phase of *N. brasiliensis* infection.

IFNγ neutralization in *Il17a*-KO mice rescues the impaired type 2 immune response

To directly test whether active suppression of IFNγ by IL-17A is required for the full development of a type 2 immune response during *N. brasiliensis* infection, IFNγ was neutralised at day -1 and 1 of infection in *Il17a*-KO mice and responses examined at day 8 post-infection. (Fig. 5A). The significant defect in eosinophilic responses in *Il17a*-KO mice compared to WT mice was still evident at day 8 post-infection. However, blocking IFNγ in *Il17a*-KO mice enhanced eosinophil numbers (Fig 5B). The same pattern was observed for numbers of $CD4^+$ T cells in the lungs (Fig. 5C). To determine whether IFNγ neutralisation altered the type 2 response, we firstly assessed expression of key type 2 cytokines *Il4* and *Il13* in the lungs of mice. Whilst expression of these genes was significantly reduced in infected *Il17a*-KO mice compared to WT mice, IFNγ depletion completely recovered expression of these cytokines in *Il17a*-KO mice compared to isotype-treated animals, and *Il4* surpassed the levels seen in WT mice (Fig. 5D). Additionally, we assessed the type 2 marker, *Chil3*, which also demonstrated enhanced expression in *Il17a*-KO mice treated with anti-IFNγ compared to similarly treated WT mice (Fig. 5E). Similarly, analysis of numbers of IL-5 and IL-13 producing $CD4^+$ T cells at d8 post infection showed restoration of the type 2 response in *Il17a*-KO mice that received the neutralising IFNγ antibody (Fig. 5F). Consistent with the ability of IFNγ to regulate type 2 cytokines, IFNγ depletion also restored the activation status of $CD4^+$ T cells in the *Il17a*-KO mice (Fig. 5G) and increased the numbers of $CD4^+$ T cells expressing type 2 markers EGFR, PD1 and ST2 (Fig. 5H). Again, no effect was observed in these parameters in IFNγ-depleted WT mice. Here, we show that an initial reduction in IFNγ levels during *N. brasiliensis* infection mediated by IL-17A, allows the subsequent development of type 2 immunity in the lung.

IL-17A suppresses an established type 2 response in the lung

IFNγ depletion in *Il17a*-KO mice not only restored the type 2 response, but in some cases exceeded WT levels. Therefore, we hypothesized that IL-17A may suppress the type 2 immune response during later stages of *N. brasiliensis* infection. To test this hypothesis, we neutralized IL-17A at d4pi, d5pi and d6pi in WT mice and assessed immune responses at d7pi (Fig. 6A). Blocking of IL-17A led to a significant increase in both ILC2 numbers and frequencies in the

lung (Fig. 6B), as well as the numbers of ILC2s producing IL-5 and IL-13 (Fig. 6C). However, $CD4^+$ T cell numbers in the lung were comparable between isotype-treated and anti-IL-17A-treated WT mice (Fig. 6D). However, the ability of CD4+ T cells to produce type 2 cytokines may partly rely on IL-17A, as mice administered anti-IL-17A showed a slight increase IL-5 and IL-13 (Fig. 6E). This data demonstrates that IL-17A can have differential effects depending on the time and status of infection. While early IL-17A promotes the type 2 response, later in infection IL-17A acts to suppress and limit excessive the type 2 immunity, particularly in ILC2s.

IL-17A does not regulate type 2 immune responses at the site of *T. muris* infection

Our data demonstrate an impairment of the type 2 immune response in the lung during infection with the lung-migrating nematode *N. brasiliensis*. To investigate whether this impairment is lung-specific and if IL-17A also regulates type 2 responses during infection with a gut-specific nematode, we infected WT and *Il17a*-KO mice with a high dose of 200 *Trichuris muris* eggs. Infection with *T. muris* begins with the ingestion of infective eggs that accumulate in the caecum. L1 larvae hatch and penetrate the caecum and proximal colon wall, undergoing moults to L2 (d9-11pi), L3 (d17pi) and L4 (d22 pi). The host type 2 immune response occurs around the time when the parasites moult to L3s at approximately d17pi. Adult worms, if not already expelled, can be found from d32pi onwards [38]. High dose *T. muris* infection is known to induce a strong type 2 response within the gastrointestinal tract, especially in the caecum and MLNs [21], [39]. Here, worm counts in the caecum of *Il17a*-KO mice and WT mice were comparable at d19pi and d32pi (Fig. 7A), indicating IL-17A does not alter parasite expulsion rate. Cell numbers in the caecum were analysed and no differences in eosinophil and neutrophil frequency were observed between *Il17a*-KO mice and WT controls on d19pi and d32pi (Supplement Fig. 3A, B), suggesting an IL-17A-independent recruitment mechanism for both these cell types. $CD4^+$ T cell numbers in the MLN were also comparable on d19pi and d32pi between *Il17a*-KO mice and WT controls (Suppl. Fig 3C). Although there was an induction of type 2 cytokines in infected mice as measured by intracellular cytokine staining, the numbers of IL-5 or IL-13-producing $CD4^+$ T cells in the MLNs did not significantly differ between the groups (Suppl. Fig 3D). Secreted levels of IL-5, IL-9 and IL-13 in MLN cells also did not show any significant differences between *Il17a*-KO mice and WT controls (Suppl. Fig 3E). Together, these data failed to provide any evidence that IL-17A was an important regulator of type 2 immunity in the intestine during *T. muris* infection.

Previous studies have shown that despite the restriction of the *T. muris* lifecycle to the gastro-intestinal tract of the mammalian host, evidence of a type 2 immune response can be observed at distant sites, such as the lung [40] . Therefore, the immune response in the lung of *T. muris* infected WT vs *Il17a*-KO mice at d19pi and d35pi was assessed. Neutrophils numbers were increased in infected WT animals at d19pi and d35pi but this was significantly reduced in *Il17a*-KO mice on d19pi (Fig. 7B). No significant changes were observed for eosinophils (Fig. 7C). Whilst lung $CD4^+$ T cell numbers in infected animals did not change compared to naïve controls (Fig. 7D), *Il17a*-KO mice had significantly fewer $IL\text{-}5^+CD4^+$ T cells at d19 and d32pi compared to WT controls (Fig. 7E). Although the effect on $IL\text{-}13^+CD4^+$ T cells was less evident, infected *Il17a*-KO mice failed to significantly increase numbers of $Il\text{-}13^+CD4^+$ T cells compared to uninfected controls (Fig. 7E). Supporting the intracellular cytokine staining, qRT-PCR analysis in whole lung tissue showed an impairment of type 2 cytokines in the *Il17a*-KO mice, with significantly decreased expression of *Il4* (d32pi) and *Il5* (d19pi) (Fig. 7F).

Similar to infection with *N. brasiliensis*, we also observed an upregulation of IFNγ in the lung during *T. muris* infection in *Il17a*-KO mice. Both the number and the frequency of $IFN\gamma^+CD4^+$ T cells in the lung were significantly increased in *Il17a*-KO compared to WT infected mice on d19pi (Fig. 7G). This data utilising *T. muris* infection models suggests that IL-17A-dependent suppression of IFNγ allows promotion of the type 2 immune response specifically in the lungs but not the intestine.

Discussion

IL-17A, the key cytokine of the IL-17 family, is central to barrier immunity, combating fungal infections and inducing antimicrobial proteins as well as neutrophil activating and recruiting chemokines [2]. Here, we explored the relationship between IL-17A and type 2 immunity during *N. brasiliensis* infection and show that IL-17A, by impinging on IFNγ expression, allows type 2 immunity to fully develop within the lung.

As expected, IL-17A was important for innate neutrophilic responses during *N. brasiliensis* infection. However, neutrophil depletion and transfer experiments demonstrated that neutrophils themselves only partly contributed to the development of type 2 immunity, mainly through enhancement of the subsequent eosinophilia. Our data highlighted a potential role for the chemokine *Ccl8* in neutrophil mediated recruitment of eosinophils. A correlation between

CCL8 and eosinophil numbers in allergic airway inflammation has been described previously [41] and CCL8 was associated with type 2 inflammatory responses in the lung during the protective response to *Klebsiella pneumonia* [42]. However, neither study demonstrated a direct eosinophil chemotactic function of CCL8. More recently, Puttur et al. revealed that CCL8 is important for the appropriate mobilisation of ILC2s and specifically the localised production of IL-5 by ILCs, possibly explaining why we observed reduced eosinophilia in neutrophil depleted mice [43]

Neutrophils have been implicated in nematode killing [44]–[46]. These studies show the importance of neutrophil influx during the skin stage of nematode infection, while in our model of lung infection, neutrophils seem to play a minor role in worm killing. However, consistent with work from Chen et al, neutrophil depletion did result in reduced lung damage d2pi, confirming early neutrophilia as a main driver of acute lung injury following *N. brasiliensis* infection [11].

The ability of type 2 cytokines to suppress IL-17 has been well documented [47]–[49], but our study suggests that the development of the type 2 response in the first place can require IL-17A. Our data is supported by a model of murine atopic dermatitis, in which Nakajima et al. show that IL-4 production is reduced by IL-17A deficiency and that *in vitro* Th2 differentiation from naïve T cells is enhanced with the addition of IL-17A [14]. Notably, the IL-17A-induced IL-4 [14] may subsequently suppress IL-17A production as a feedback mechanism, consistent with the previous observations that type 2 cytokines negatively regulate IL-17A [50]. In allergic airway inflammation models, deficiency of IL-17A also leads to decreased type 2 cytokine production [15] and Th17 cells contribute to Th2-cell-mediated eosinophilic airway inflammation [51]. A combination of type 2 cytokines and IL-17A can be also found as signature for severe disease pathology. For example in a model for severe airway hyperresponsiveness, IL-17A contributes to asthma pathology by enhancing IL-13 activity [52]. Furthermore, during murine and human schistosomiasis and onchocerciasis, a dysregulated balance between IL-17A and type 2 responses can exacerbate the pathology [4]–[6], [53].

In our effort to understand how IL-17A might be required for full type 2 immunity, we identified a role for IL-17A mediated suppression of IFNγ. Evidence that IL-17A can regulate

IFNγ exists in the literature, but whether IFNγ is upregulated or downregulated is controversial and likely depends on the setting, timing and location [54]–[56]. During experimental visceral leishmaniasis, *Il17a*-KO mice have enhanced production of a protective IFNγ response [54], while in *Toxoplasma gondii* infection, excessive IFNγ in *Il17a*-KO mice has severe pathological consequences [55]. Evidence also exists in the context of helminth infection, where a lack of IL-17A drives elevated IFNγ during infection with the filarial nematode *Litomosoides sigmondontis* [57] or *Schistosoma japonicum* [56] and *Schistosoma mansoni* [5]. Together these findings support a potentially widespread role for IL-17A in regulating IFNγ.

Our study shows that early in infection, IL-17A suppression of IFNγ in the lung has consequences for the subsequent development of type 2 immune responses. Notably, in *Il17a*-KO mice the protective type 2 immune response in the small intestine was not impaired as mice were still able to expel *N. brasiliensis*. To examine whether IL-17A-dependent regulation of IFNγ is site specific, we used high dose infection with the colon dwelling parasite *T. muris*. The protective type 2 immune response against *T. muris* in the intestine was intact in mice lacking IL-17A. The surprising finding however was that even though *T. muris* does not have a lung stage, the concurrent type 2 response in the lung was impaired in *Il17a*-KO mice. $CD4^+$ T cells in the lung produced less type 2 cytokines and both eosinophils and neutrophils were significantly downregulated in the *Il17a*-KO mice. Consistent with our findings in *N. brasiliensis*, $CD4^+$ T cells in *Il17a-KO* mice produced significantly higher amounts of IFNγ than in their WT counterparts. Together, our data suggest that the impact of IL-17A on type 2 development may be lung restricted. Nonetheless, there may still be a fundamental requirement for IFNγ suppression for type 2 immunity to progress. Artis et al. demonstrated that the type 2 immune response during *T. muris* requires TSLP, and in very similar experiments to those described here, demonstrated that TSLP functions to suppress IFNγ [58]. Thus, early suppression of IFNγ may be a general pre-requisite for the development of a type 2 environment with a requirement for IL-17A in the lung and TSLP (or other factors) in the gut.

Our data also reveal a potential time dependence on the regulation of type 2 immunity by IL-17A. While the early γδ T cell-derived IL-17A supported the type 2 response, late IL-17A, derived from both Th17 cells and γδ T cells, appeared to be a negative regulator. We observed that depletion of early IFNγ in *Il17a*-KO mice not only rescued their impaired type 2 immune responses on d8pi, but the type 2 mRNA signature significantly exceeded the WT levels. Thus,

555 removal of IFNγ in IL-17A deficient mice, which allowed normal type 2 progression, revealed a potential role for IL-17A in suppressing type 2 cytokines. To our knowledge, IL-17A suppression of type 2 cytokines has not previously been described in vivo.

We have not yet addressed the full mechanism behind IL-17A-mediated suppression of IFNγ 560 during *N. brasiliensis* infection but it is notable that IL-17A not only impairs type 2 cytokine production, but also alters the cellular activation status and expression of type 2 markers. Interestingly, in our model, we only observe impairment of type 2 immune responses in the lung itself and not in the Th2 cells from lung-draining lymph nodes. Expression of EGFR and ST2, two markers closely associated with type 2 settings [29], were reduced on the $CD4^+$ T 565 cells of *Il17a*-KO mice in the lung. EGFR expression on Th2 cells is critical for resistance during GI helminth infection and a signalling complex between EGFR and ST2 can activate Th2 cells to secrete IL-13 in an antigen-dependent manner upon IL-33 exposure. Our data would suggest that this "licensing" of Th2 cells does not occur in the *Il17a*-KO mice during *N. brasiliensis* infection, indicating that IL-17A is needed for a proper induction of the adaptive 570 Th2 response in the lung.

Together we demonstrate that the early events in the lung shape the protective type 2 immune response, with IL-17A as a critical regulator through the downregulation of IFNγ. In combination with previous data [58], suppression of IFNγ at barrier sites may be a central paradigm for type 2 immunity. The ability of IL-17A to subsequently suppress type 2 575 responses reveal an important feedback loop that must go awry during severe asthma and other type 2 conditions, in which IL-17 plays a damaging and pathogenic role.

Acknowledgments

We thank the Flow Cytometry, Bioimaging, and Biological Services core facilities at the 580 University of Manchester. This work was supported by the Wellcome Trust (106898/A/15/Z to JEA and Z10661/Z/18/Z to RG), the Medical Research Council UK (MR/K01207X/1 to JEA), Medical Research Foundation UK joint funding with Asthma UK (MRFAUK-2015-302 to TES). SC was supported by a Wellcome Trust Studentship (103132/Z/13/Z). We thank Kevin Couper for CD45.1 mice.

585 **Disclosures**

The authors have no financial conflicts of interest.

References

[1] P. H. Papotto, J. C. Ribot, and B. Silva-Santos, "IL-17 + γδ T cells as kick-starters of
590 inflammation," *Nature Immunology*, vol. 18, no. 6. Nature Publishing Group, pp. 604–611, 18-May-2017.

[2] Y. Iwakura, H. Ishigame, S. Saijo, and S. Nakae, "Functional Specialization of Interleukin-17 Family Members," *Immunity*, vol. 34, no. 2. pp. 149–162, 25-Feb-2011.

[3] J. E. Allen and R. M. Maizels, "Diversity and dialogue in immunity to helminths,"
595 *Nat. Rev. Immunol.*, 2011.

[4] M. Mbow *et al.*, "T-helper 17 cells are associated with pathology in human schistosomiasis," *J. Infect. Dis.*, vol. 207, no. 1, pp. 186–195, 2013.

[5] L. I. Rutitzky and M. J. Stadecker, "Exacerbated egg-induced immunopathology in murine Schistosoma mansoni infection is primarily mediated by IL-17 and restrained
600 by IFN-γ," *Eur. J. Immunol.*, 2011.

[6] G. Katawa *et al.*, "Hyperreactive Onchocerciasis is Characterized by a Combination of Th17-Th2 Immune Responses and Reduced Regulatory T Cells," *PLoS Negl. Trop. Dis.*, 2015.

[7] D. F. Choy *et al.*, "T_H2 and T_H7 inflammatory pathways are reciprocally regulated in
605 asthma," *Sci. Transl. Med.*, 2015.

[8] T. E. Sutherland *et al.*, "Chitinase-like proteins promote IL-17-mediated neutrophilia in a tradeoff between nematode killing and host damage.," *Nat. Immunol.*, vol. 15, no.

12, pp. 1116–25, 2014.

[9] A. B. Molofsky *et al.*, "InterleuKin-33 And Interferon-Γ Counter-Regulate Group 2 Innate Lymphoid Cell Activation During Immune Perturbation," *Immunity*, vol. 43, no. 1, pp. 161–174, Jul. 2015.

[10] D. C. Newcomb *et al.*, " A Functional IL-13 Receptor Is Expressed on Polarized Murine CD4 + Th17 Cells and IL-13 Signaling Attenuates Th17 Cytokine Production ," *J. Immunol.*, 2009.

[11] F. Chen *et al.*, "Neutrophils prime a long-lived effector macrophage phenotype that mediates accelerated helminth expulsion.," *Nat. Immunol.*, vol. 15, no. 10, pp. 938–46, 2014.

[12] F. Chen *et al.*, "Neutrophils prime a long-lived effector macrophage phenotype that mediates accelerated helminth expulsion," *Nat. Immunol.*, vol. 15, no. 10, pp. 938–946, Jan. 2014.

[13] T. E. Sutherland, D. Rückerl, N. Logan, S. Duncan, T. A. Wynn, and J. E. Allen, "Ym1 induces RELMα and rescues IL-4Rα deficiency in lung repair during nematode infection," *PLoS Pathog.*, 2018.

[14] S. Nakajima *et al.*, "IL-17A as an inducer for Th2 immune responses in murine atopic dermatitis models," *J. Invest. Dermatol.*, vol. 134, no. 8, pp. 2122–2130, 2014.

[15] S. Nakae *et al.*, "Antigen-specific T cell sensitization is impaired in Il-17-deficient mice, causing suppression of allergic cellular and humoral responses," *Immunity*, vol. 17, no. 3, pp. 375–387, Sep. 2002.

[16] P. Chenuet *et al.*, "Neutralization of either IL-17A or IL-17F is sufficient to inhibit house dust mite induced allergic asthma in mice," *Clin. Sci.*, 2017.

[17] S. Srinivas *et al.*, "Cre reporter strains produced by targeted insertion of EYFP and

ECFP into the ROSA26 locus," *BMC Dev. Biol.*, 2001.

[18] K. Hirota *et al.*, "Fate mapping of IL-17-producing T cells in inflammatory responses," *Nat. Immunol.*, 2011.

[19] R. A. Lawrence, C. A. Gray, J. Osborne, and R. M. Maizels, "Nippostrongylus brasiliensis: Cytokine responses and nematode expulsion in normal and IL-4 deficient mice," *Exp. Parasitol.*, 1996.

[20] M. J. Holland, Y. M. Harcus, P. L. Riches, and R. M. Maizels, "Proteins secreted by the parasitic nematode Nippostrongylus brasiliensis act as adjuvants for Th2 responses," *Eur. J. Immunol.*, 2000.

[21] A. J. Bancroft, A. N. McKenzie, and R. K. Grencis, "A critical role for IL-13 in resistance to intestinal nematode infection.," *J. Immunol.*, 1998.

[22] M. Swamydas, Y. Luo, M. E. Dorf, and M. S. Lionakis, "Isolation of mouse neutrophils," *Curr. Protoc. Immunol.*, vol. 2015, pp. 3.20.1-3.20.15, 2015.

[23] K. S. Hayes *et al.*, "Chronic Trichuris muris infection causes neoplastic change in the intestine and exacerbates tumour formation in APC min/+ mice," *PLoS Negl. Trop. Dis.*, 2017.

[24] R Core Team, "R Core Team (2015). R: A language and environment for statistical computing.," *R Found. Stat. Comput. Vienna, Austria. URL http//www.R-project.org/.*, 2015.

[25] R. MD, M. DJ, and S. GK, "edgeR: a Bioconductor package for differential expression analysis of digital gene expression data," *Bioinformatics*, 2009.

[26] Z. Gu, R. Eils, and M. Schlesner, "Complex heatmaps reveal patterns and correlations in multidimensional genomic data," *Bioinformatics*, 2016.

[27] H. Wickham, "tidyverse: Easily Install and Load 'Tidyverse' Packages.," 2016.

[28] L. Campbell *et al.*, "ILC2s mediate systemic innate protection by priming mucus production at distal mucosal sites," *J. Exp. Med.*, 2019.

[29] C. M. Minutti *et al.*, "Epidermal Growth Factor Receptor Expression Licenses Type-2 Helper T Cells to Function in a T Cell Receptor-Independent Fashion," *Immunity*, 2017.

[30] S. A. Redpath *et al.*, "ICOS controls Foxp3+ regulatory T-cell expansion, maintenance and IL-10 production during helminth infection," *Eur. J. Immunol.*, vol. 43, no. 3, pp. 705–715, 2013.

[31] L. I. Terrazas, D. Montero, C. A. Terrazas, J. L. Reyes, and M. Rodríguez-Sosa, "Role of the programmed Death-1 pathway in the suppressive activity of alternatively activated macrophages in experimental cysticercosis," *Int. J. Parasitol.*, 2005.

[32] C. Nembrini, B. J. Marsland, and M. Kopf, "IL-17-producing T cells in lung immunity and inflammation," *Journal of Allergy and Clinical Immunology*. 2009.

[33] A. Porzionato *et al.*, "Fractal analysis of alveolarization in hyperoxia-induced rat models of bronchopulmonary dysplasia," *Am. J. Physiol. Cell. Mol. Physiol.*, 2016.

[34] J. E. Allen, "Inflammasome-independent role for NLRP3 in controlling innate anti-helminth immunity and tissue repair in the lung," pp. 1–32, 2019.

[35] A. Ardain *et al.*, "Group 3 innate lymphoid cells mediate early protective immunity against tuberculosis," *Nature*. 2019.

[36] L. C. Osborne *et al.*, "Coinfection. Virus-helminth coinfection reveals a microbiota-independent mechanism of immunomodulation," *Science (80-.).*, vol. 345, no. 6196, pp. 578–582, 2014.

[37] J. C. Ribot *et al.*, "CD27 is a thymic determinant of the balance between interferon-γ- and interleukin 17-producing γδ T cell subsets," *Nat. Immunol.*, 2009.

[38] J. E. Klementowicz, M. A. Travis, and R. K. Grencis, "Trichuris muris: A model of gastrointestinal parasite infection," *Seminars in Immunopathology*. 2012.

[39] A. J. Bancroft, K. J. Else, and R. K. Grencis, "Low-level infection with Trichuris muris significantly affects the polarization of the CD4 response," *Eur. J. Immunol.*, 1994.

[40] K. J. Filbey *et al.*, "Intestinal helminth infection promotes IL-5- and CD4 + T cell-dependent immunity in the lung against migrating parasites," *Mucosal Immunol.*, 2019.

[41] J. L. Costa Carvalho *et al.*, "The chemokines secretion and the oxidative stress are targets of low-level laser therapy in allergic lung inflammation," *J. Biophotonics*, 2016.

[42] D. E. Dulek *et al.*, "Allergic airway inflammation decreases lung bacterial burden following acute Klebsiella pneumoniae infection in a neutrophil- and CCL8-dependent manner," *Infect. Immun.*, 2014.

[43] F. Puttur *et al.*, "Pulmonary environmental cues drive group 2 innate lymphoid cell dynamics in mice and humans," *Sci. Immunol.*, 2019.

[44] S. Bonne-Année *et al.*, "Extracellular traps are associated with human and mouse neutrophil and macrophage mediated killing of larval Strongyloides stercoralis," *Microbes Infect.*, vol. 16, no. 6, pp. 502–511, 2014.

[45] J. Ajendra *et al.*, "NOD2 dependent neutrophil recruitment is required for early protective immune responses against infectious Litomosoides sigmodontis L3 larvae.," *Sci. Rep.*, vol. 6, p. 39648, 2016.

[46] T. E. Sutherland *et al.*, "Chitinase-like proteins promote IL-17-mediated neutrophilia in a tradeoff between nematode killing and host damage," *Nat. Immunol.*, vol. 15, no. 12, pp. 1116–1125, Nov. 2014.

[47] D. C. Newcomb *et al.*, "IL-13 Regulates Th17 Secretion of IL-17A in an IL-10–Dependent Manner," *J. Immunol.*, 2012.

[48] S. J. Van Dyken *et al.*, "Chitin activates parallel immune modules that direct distinct inflammatory responses via innate lymphoid type 2 and γδ T cells," *Immunity*, 2014.

[49] F. Chen *et al.*, "An essential role for T H 2-type responses in limiting acute tissue damage during experimental helminth infection," *Nat. Med.*, vol. 18, no. 2, pp. 260–266, Feb. 2012.

[50] K. Eyerich *et al.*, "IL-17 in atopic eczema: Linking allergen-specific adaptive and microbial-triggered innate immune response," *J. Allergy Clin. Immunol.*, 2009.

[51] H. Wakashin, K. Hirose, I. Iwamoto, and H. Nakajima, "Role of IL-23-Th17 cell axis in allergic airway inflammation," in *International Archives of Allergy and Immunology*, 2009.

[52] S. Lajoie *et al.*, "Complement-mediated regulation of the IL-17A axis is a central genetic determinant of the severity of experimental allergic asthma," *Nat. Immunol.*, 2010.

[53] A. Díaz and J. E. Allen, "Mapping immune response profiles: The emerging scenario from helminth immunology," *European Journal of Immunology*. 2007.

[54] C. Terrazas, S. Varikuti, J. Kimble, E. Moretti, P. N. Boyaka, and A. R. Satoskar, "IL-17A promotes susceptibility during experimental visceral leishmaniasis caused by Leishmania donovani," *FASEB Journal*, vol. 30, no. 3. pp. 1135–1143, 2016.

[55] M. Moroda, M. Takamoto, Y. Iwakura, J. Nakayama, and F. Aosai, "Interleukin-

17Adeficient mice are highly susceptible to Toxoplasma gondii infection due to excessively induced T. gondii HSP70 and interferon gamma production," *Infect. Immun.*, 2017.

[56] Y. Zhang *et al.*, "Lack of IL-17 signaling decreases liver fibrosis in murine schistosomiasis japonica," *Int. Immunol.*, 2015.

[57] M. Ritter *et al.*, "Absence of IL-17A in Litomosoides sigmodontis-infected mice influences worm development and drives elevated filarial-specific IFN-γ," *Parasitol. Res.*, 2018.

[58] B. C. Taylor *et al.*, "TSLP regulates intestinal immunity and inflammation in mouse models of helminth infection and colitis," *J. Exp. Med.*, 2009.

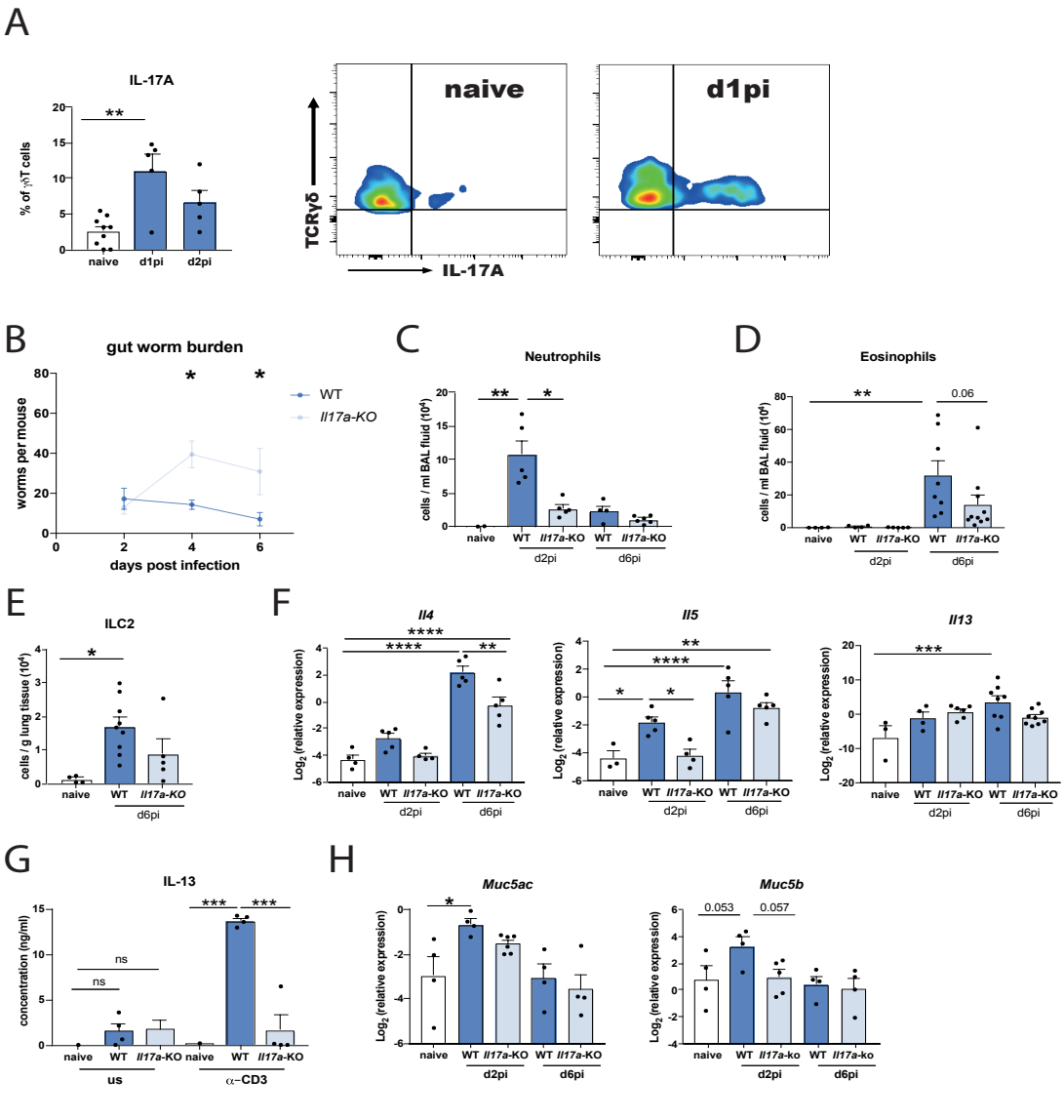

Figure 1: Mice deficient in IL-17A mount a diminished type 2 response at the site of infection

C57BL6/J (WT) and *Il17a*-KO mice were infected with 250 *N. brasiliensis* L3's and cell frequencies and cytokines were measured at different time points post infection. Frequencies of IL-17A producing γδ T cells on d1pi and d2pi and representative flow-plot at d1pi (**A**). Worm burden in small intestine assessed in WT and *Il17a*-KO mice on days 2, 4 and 6 post *N. brasiliensis* infection (**B**). Absolute count of neutrophils ($Ly6G^+CD11b^+$) (**C**), eosinophils ($SiglecF^+CD11b^+$ $Cd11c^-$) in bronchoalveolar lavage (BAL) (**D**) and lung ILC2 (Lineage-KLRG+CD127+CD90.2+ST2+) as measured via flow cytometry (**E**). Relative mRNA expression of cytokines *Il4*, *Il5* and *Il13* in whole lung as quantified by qRT-PCR (log2 expression relative to *actb* (β-actin)) (**F**). IL-13 levels from unstimulated or 72h α-CD3 treated single-suspension lung cells (**G**). Relative mRNA expression of the mucin genes *Muc5ac* and *Muc5b* in whole lung (log_2 expression relative to *actb*) (**G**). Data are representative (mean ± s.e.m.) of at least 3 individual experiments (A, C, E-F) or pooled of two experiments (D, G, H) with at least 3 mice per group or pooled data from three experiments (B). Data were tested for normality using Shapiro-Wilk test and analysed using One-Way Anova followed by Sidak's multiple comparisons test for selected groups. NS – not significant. Data in (**F, H)** were log2 transformed and statistical tests were performed on transformed data *P<0.05, **P<0.01, ***P<0.001, ****P<0.0001

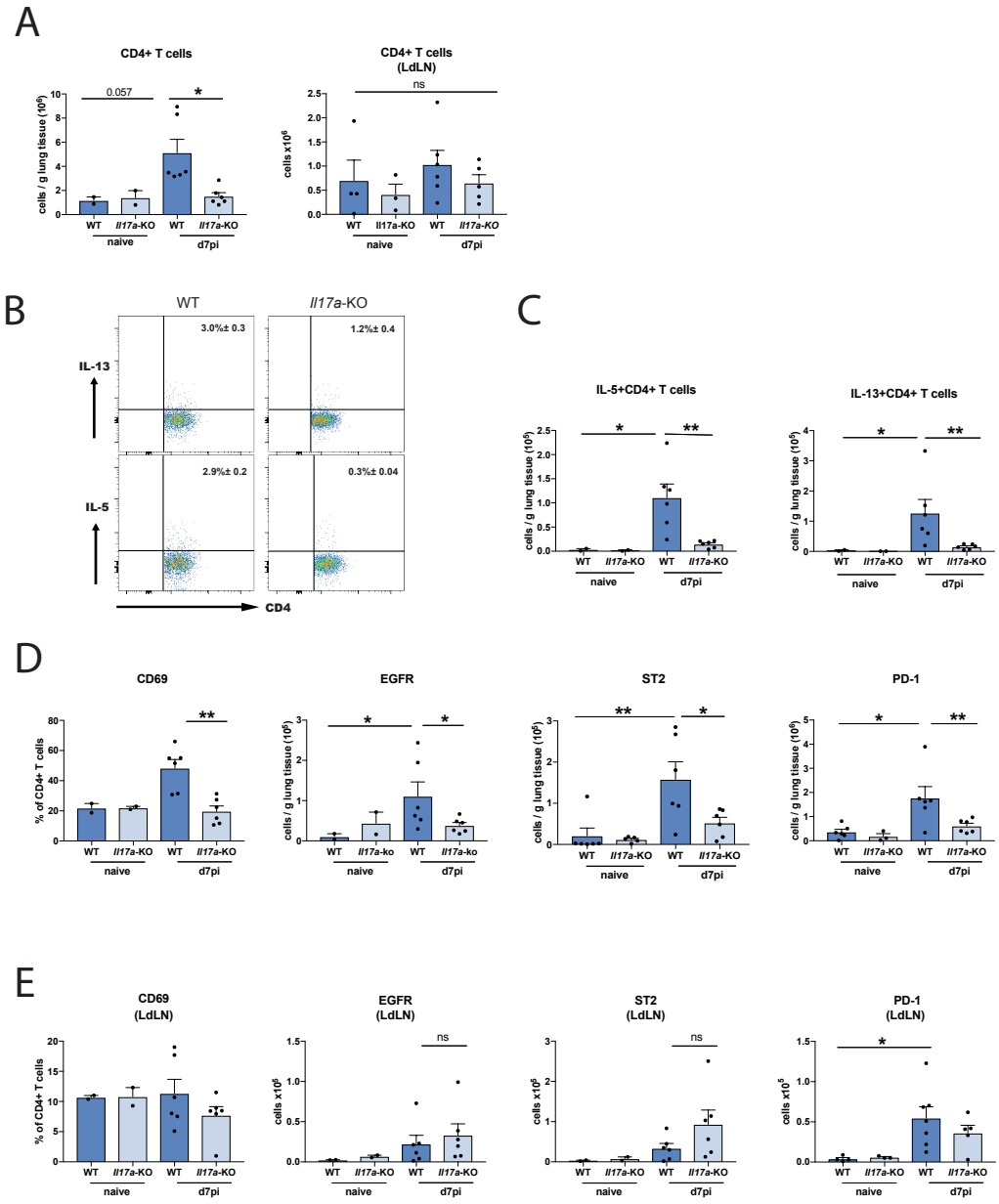

Figure 2: IL-17A regulates T cell activation and polarization during *N. brasiliensis* infection.

C57BL6/J (WT) and *Il17a-KO* mice were infected with 250 *N. brasiliensis* L3 larvae and live, single CD4$^+$ T cells were phenotyped using flow cytometry at d7pi in lung and lung draining lymph nodes (LdLN). Absolute numbers of live CD4$^+$ T cells in lung tissue and LdLN (**A**). Representative flow-plots showing frequencies of IL-5 and IL-13 production by CD4+ T cells d7pi in lung from WT *Il17a-KO* mice (**B**). Absolute numbers of IL-5$^+$ and IL-13$^+$ CD4$^+$ T cells in the lung (**C**). Expression of CD69, absolute numbers for EGFR, ST2 and PD-1 in lung (**D**) and LdLNs (**E**). Data are representative (mean ± s.e.m.) of at least 3 individual experiments with at least n=2 mice in control groups and n=4 mice in infected groups (per experiment). Data was tested for normality using Shapiro-Wilk test and analysed using One-Way Anova followed by Sidak's multiple comparisons test for selected groups. NS not significant, **P*<0.05, ***P*<0.01.

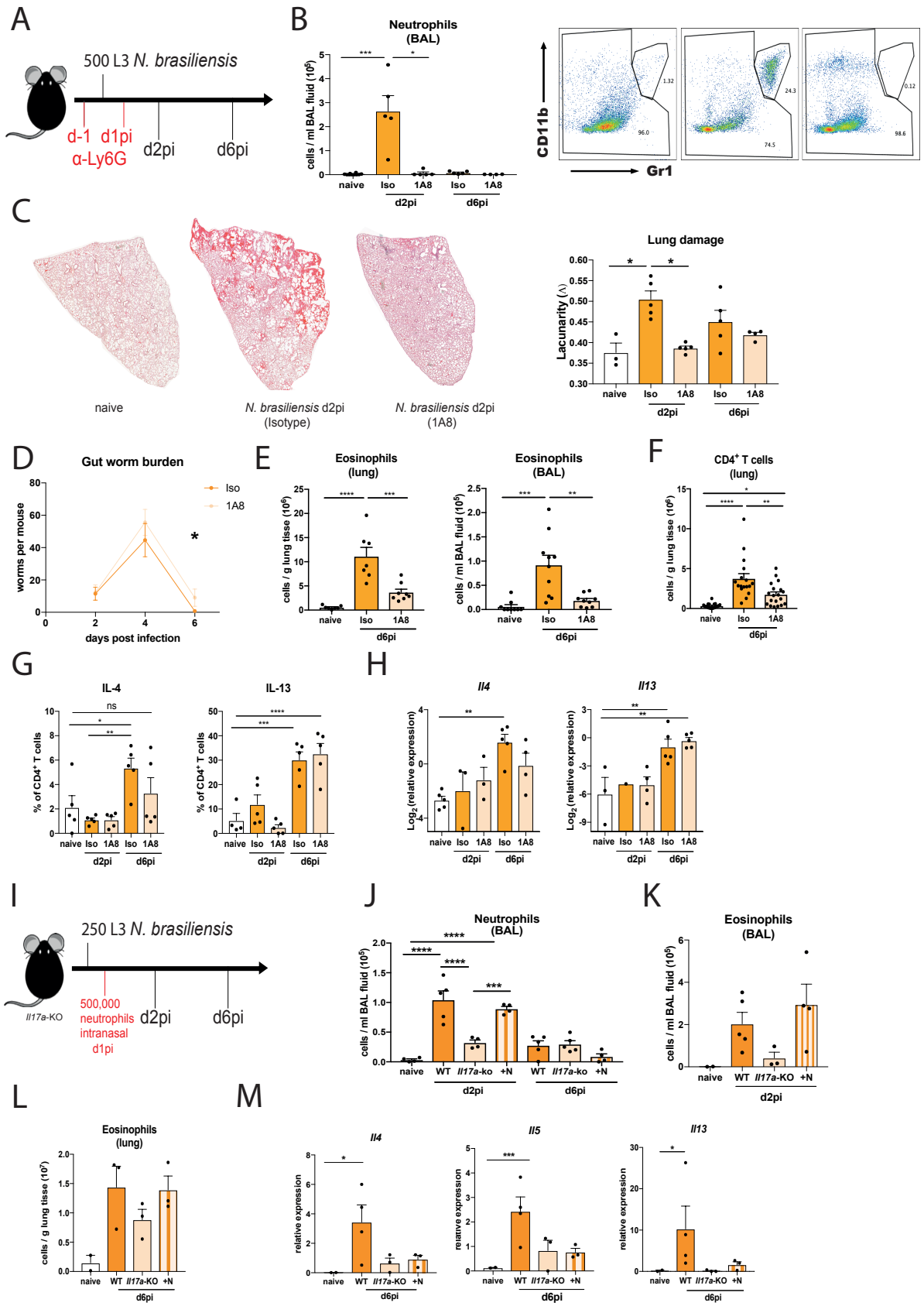

835

Figure 3: Neutrophils regulate eosinophils but not the type 2 response.
C57BL6/J mice were infected with 500 *N. brasiliensis* L3 larvae and mice were injected with α-Ly6G (1A8) or isotype control on d-1 and d1pi (**A**). Neutrophil numbers per ml BAL fluid, as well as confirmation of neutrophil depletion via flow cytometry (**B**). Representative lung sections stained with haematoxylin & eosin and imaged, followed by quantification of lacunarity (Λ) on d2pi and d6pi (**C**). Gut worm burden after neutrophil depletion d2pi, d4pi and d6pi (**D**). Eosinophils in lung and BAL (**E**) as well as $CD4^+$ T cells in lung (**F**) on d2pi and d6pi as assessed by flow cytometry. Frequencies of intracellular IL-4 and IL-13 from $CD4^+$ T cells in lung (**G**). Relative expression of *Il4* and *Il13* in total lung mRNA (log2 expression relative to *actb* (β-actin)) (**H**). *Il17a*-KO mice were intranasally injected with 500,000 neutrophils (+N) d1pi with 250 L3 larvae *N. brasiliensis*, controls received PBS (**I**). BAL neutrophils numbers on days 2 and 6 post infection with *N. brasiliensis* (**J**). Eosinophil numbers in BAL per gram lung tissue after neutrophil transfer (**K**). Relative expression of *Il4*, *Il5*, and *Il13* in whole lung mRNA in WT, *Il17a*-KO or *Il17a*-KO mice + neutrophils (+N) (**L**). Data are expressed as (mean ± s.e.m.) and are representative of at least 3 individual experiments with at least 3 mice per group (**B, C, E, J-L**) or pooled data from two experiments (**D, F**). Data were tested for normality using Shapiro-Wilk test and analysed using One-Way Anova followed by Sidak's multiple comparisons test for selected groups. **P*<0.05, ***P*<0.01, ****P*<0.001, *****P*<0.0001.

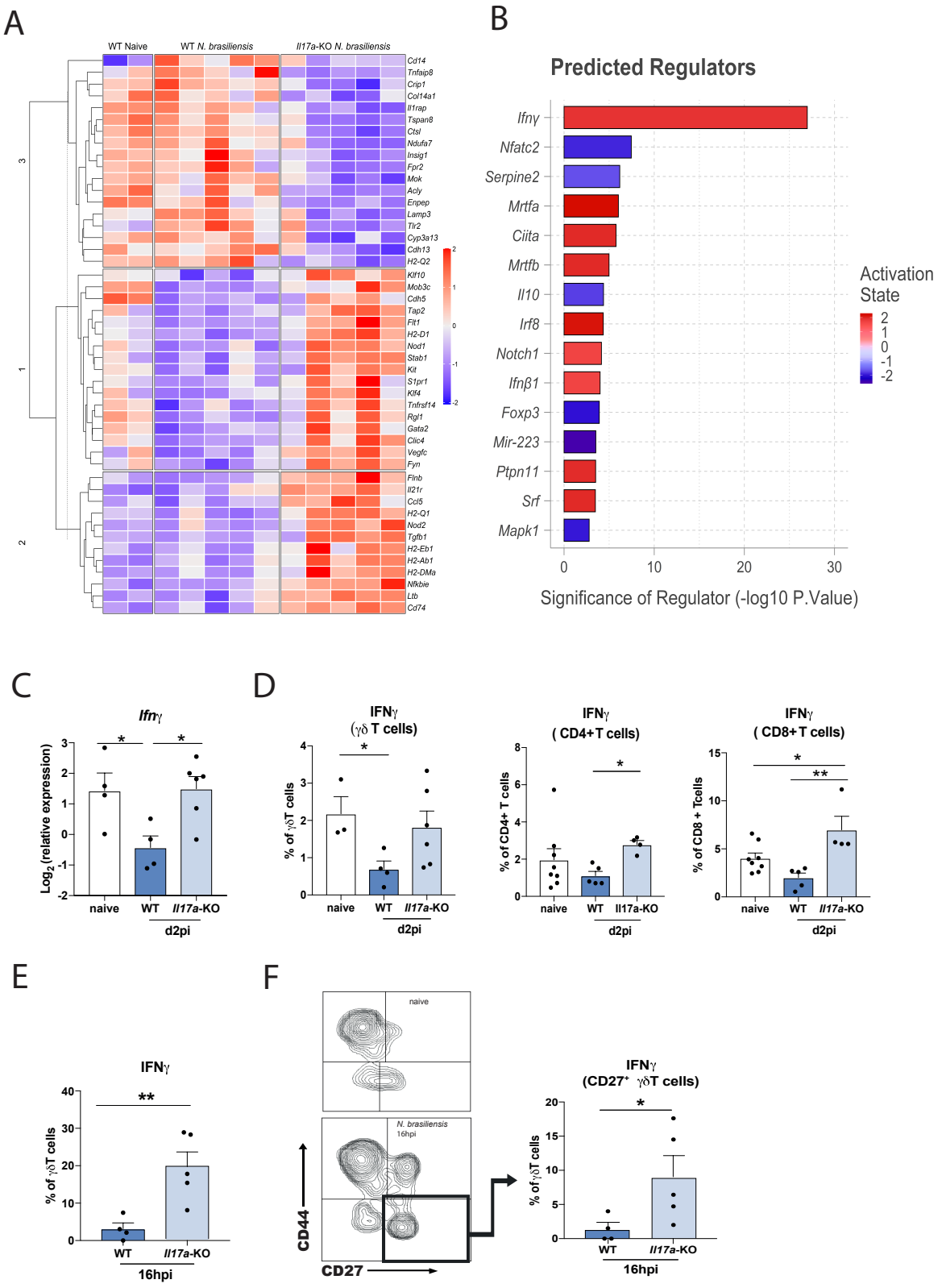

Figure 4: Presence of IL-17A leads to a downregulation of early IFNγ during *N. brasiliensis* infection.

Whole lung RNA from C57BL6/J (WT) and *Il17a*-KO mice on d2pi with *N. brasiliensis* was analysed by Nanostring. Unsupervised, hierarchically clustered heat map showing differentially expressed genes between infected WT and *Il17a*-KO mice (**A**). Top differentially regulated genes between infected WT and *Il17a*-KO mice were run in Ingenuity pathway analyzer, with top predicted regulators shown in (**B**). Relative expression of *Ifng* in whole lung of naïve WT and WT and *Il17a*-KO mice d2pi with *N. brasiliensis* (log2 expression relative to *actb* (β-actin)*)* (**C**). Frequency of IFNγ by γδ T cells, $CD4^+$ T cells, $CD8^+$ T cells in WT and *Il17a*-KO mice d2pi assessed by flow cytometry (**D**). Frequency of $IFN\gamma^+$ γδ T cells 16h post *N. brasiliensis* infection in WT and *Il17a*-KO mice (**E**). Representative flow plot showing γδ T cell subsets using CD44 and CD27 in naïve WT mice and *Il17a*-KO mice 16h post *N. brasiliensis* infection as well as frequency of $IFN\gamma^+$ $CD27^+$ γδ T cells 16h post *N. brasiliensis* infection in WT and *Il17a*-KO mice (**F**). Data (**C-F**) are expressed as (mean ± s.e.m.) and are representative of at least 2 individual experiments with at least 3 mice per infected group. Data were tested for normality using Shapiro-Wilk test and analysed using One-Way Anova followed by Sidak's multiple comparisons test for selected groups or student's t-test. $*P<0.05$, $**P<0.01$

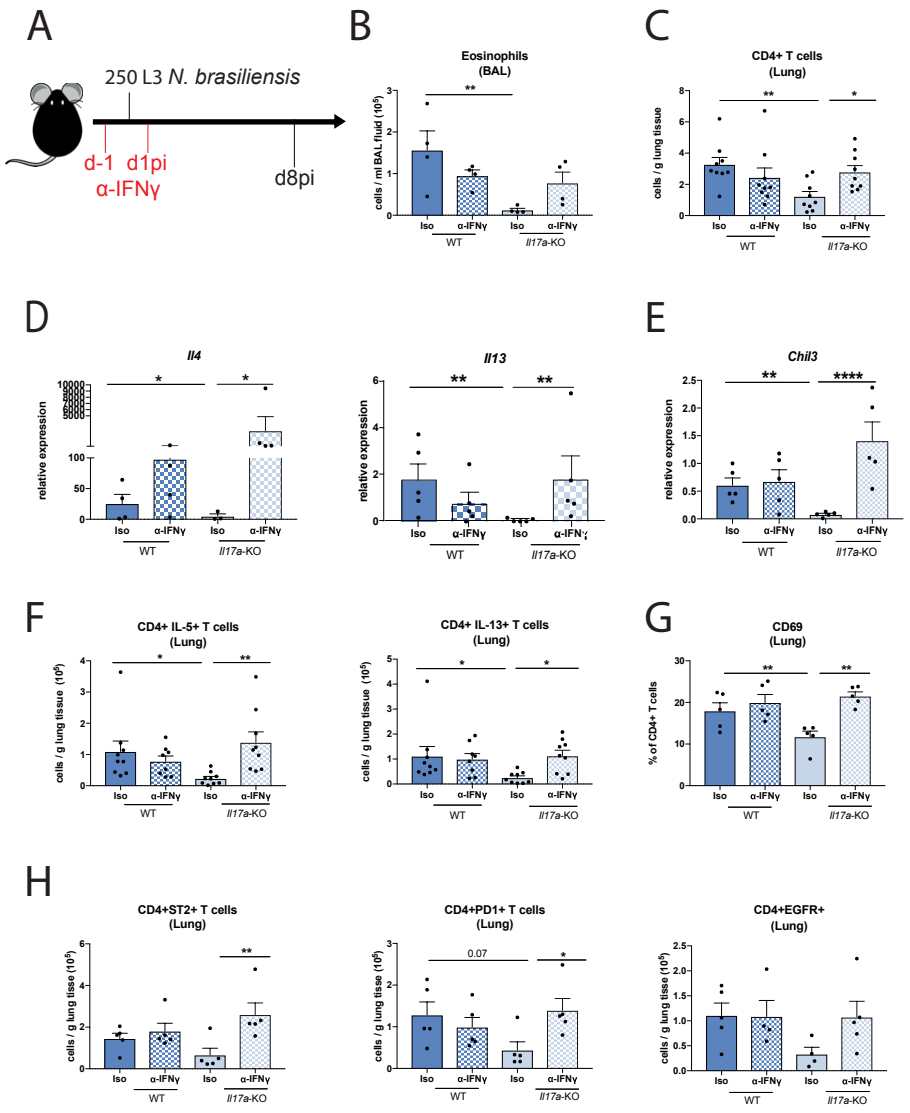

Figure 5: IFNγ neutralization in *Il17a*-KO mice rescues the impaired type 2 immune response.

C57BL6/J (WT) and *Il17a*-KO mice and were treated with α-IFNγ or isotype control on days -1 and 1pi with 250 L3 larvae of *N. brasiliensis* (**A**). Absolute cell counts of eosinophils in BAL (**B**) and CD4$^+$ T cells per gram lung tissue (**C**) as measured via flow cytometry on d8pi. Relative expression of type 2 cytokines *Il4* and *Il13* (**D**) and type 2 marker *Chil3* (**E**) from whole lung RNA. Absolute numbers of IL-5$^+$ and IL-13$^+$ CD4$^+$ T cells (**F**). Frequency of CD69 expression in CD4$^+$ T cells (**G**) and numbers of EGFR+, ST2+ and PD1+ CD4$^+$ T cells per gram lung tissue (**H**). Data (B, D, E, F, G) are representative (mean ± s.e.m.) 2 individual experiments with at least 3 mice per group (per experiment) or pooled data from two experiments (C, F). Data was tested for normality using Shapiro-Wilk test and analysed using One-Way Anova followed by Sidak's multiple comparisons test for selected groups. Data in (**D, E**) were log2 transformed and statistical tests were performed on transformed data. **P*<0.05.

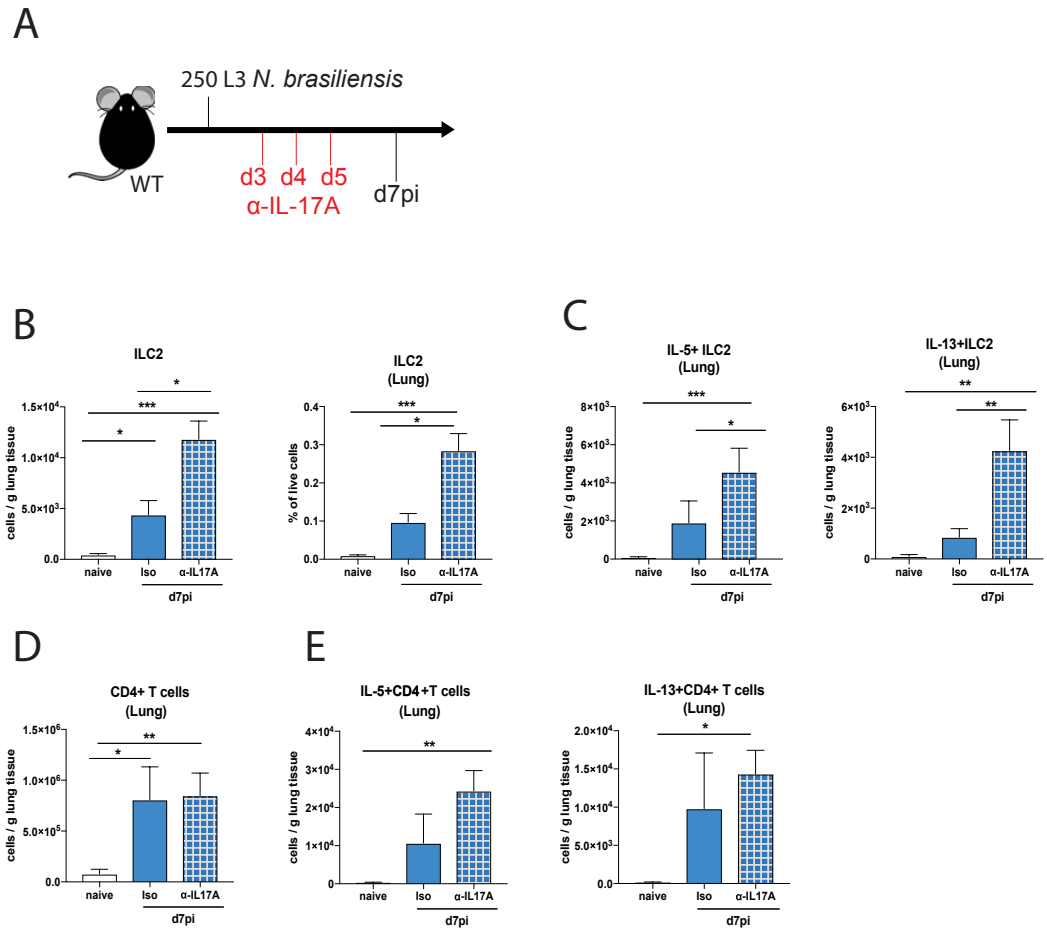

Figure 6: Late stage IL-17A suppresses type 2 immune responses. C57Bl/6 WT mice were treated with α-IL-17A or isotype control on days 3, 4, and 5pi with 250 L3 *N. brasiliensis* (**A**). Cells per gram lung tissue and frequency of ILC2 within live lung cells (**B**). Number of IL-5$^+$ and IL-13$^+$ ILC2 per gram lung tissue (n=5 for naïve, n=11-12 for d7 *N. brasiliensis* infected groups) (**C**). Numbers of CD4$^+$ T cells (**D**) and IL-5$^+$ and IL-13$^+$ CD4$^+$ T cells per gram of lung tissue (n=3 for naïve and n=6 for d7 *N. brasiliensis* infected groups) (**E**). Data pooled from two independent experiments (**B**, **C**) or are representative (mean ± s.e.m.) of 3 individual experiments with at least 3 mice per group (per experiment) (**D**, **E**). Data was tested for normality using Shapiro-Wilk test and analysed using One-Way Anova followed by Sidak's multiple comparisons test for selected groups or student's t-test. *P<0.05, **P<0.01.

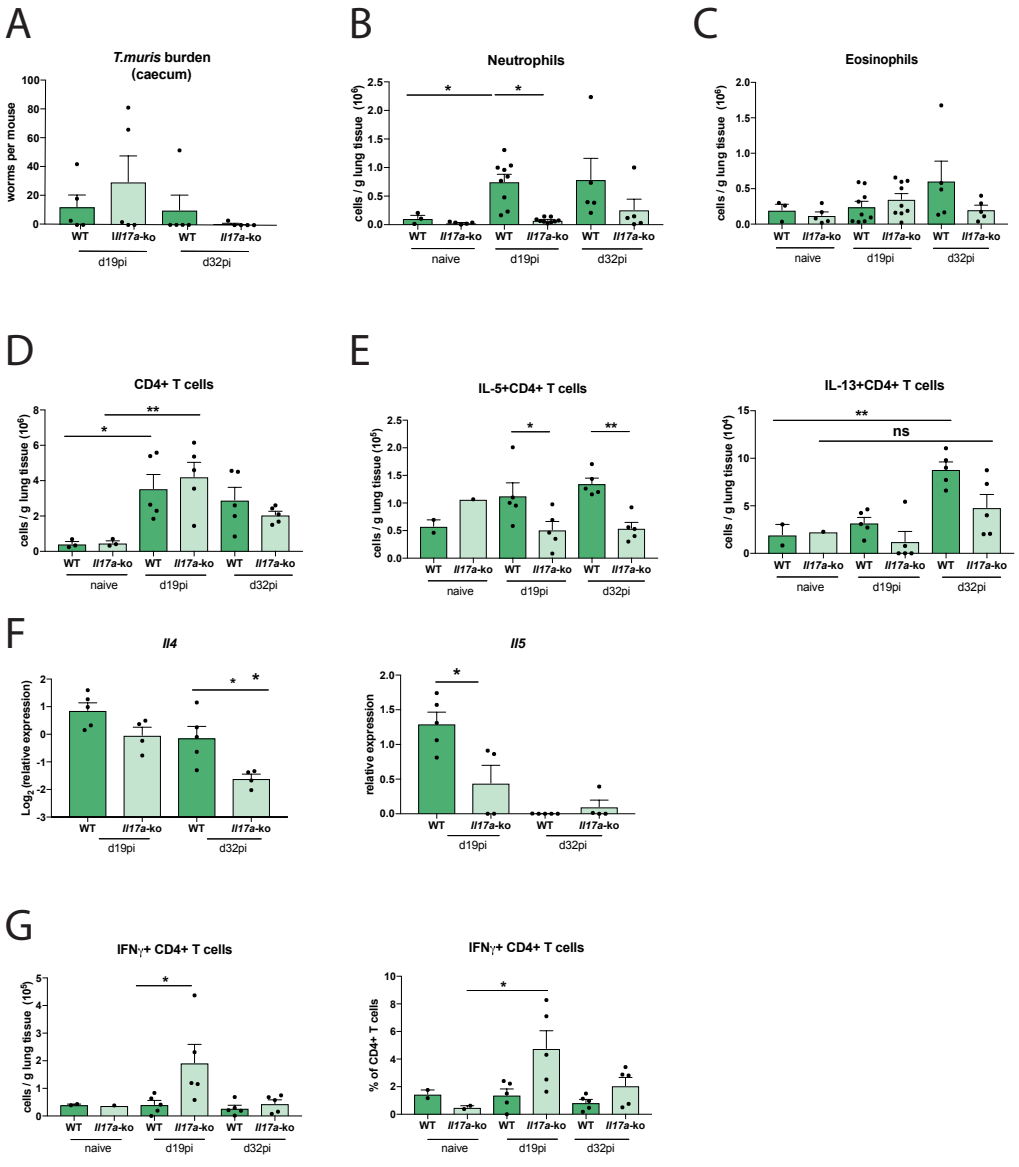

Figure 7: Lack of IL-17A impairs concurrent type 2 immune responses in the lung during infection with *Trichuris muris*.

C57Bl/6 WT and *Il17a*-KO mice were infected with a high dose of *T. muris* and immune parameters were investigated at d19 and d32pi. Worms counts in the caecum (**A**). Frequency of neutrophils (**B**), eosinophils (**C**) and CD4$^+$ T cells (**D**) in the lung at d19pi and d32pi. Absolute counts of IL-5$^+$ and IL-13$^+$ CD4+ T cells per gram of lung tissue (**E**). Relative expression of cytokines *Il4* and *Il5* from whole lung RNA (log2 expression relative to *actb* (β-actin)) (**F**). Absolute cell counts and frequency of IFNγ by CD4$^+$ T cells per gram of lung tissue (**G**). Data are expressed as mean ± s.e.m.) and are representative of 3 individual experiments with at least 4 mice per infected group and one mouse per control group. Data was tested for normality using Shapiro-Wilk test and analysed using One-Way Anova followed by Sidak's multiple comparisons test for selected groups or student's t-test. *P<0.05, **P<0.01